

SUPPORTING INFORMATION

Chemistry of group 5 metallaboranes with heterocyclic thiol ligands: a combined experimental and theoretical study

*Rini Prakash,^{#a} Anagha Haridas,^{#a} K. Bakthavachalam,^a Thierry Roisnel,^b Jean-François Halet^{*b,c} and Sundargopal Ghosh^{*a}*

^a*Department of Chemistry, Indian Institute of Technology Madras, Chennai 600036, India. E-mail: sghosh@iitm.ac.in*

^b*Univ Rennes, CNRS, Institut des Sciences Chimiques de Rennes, UMR 6226, F-35000 Rennes, France. E-mail: Jean-Francois.Halet@univ-rennes1.fr*

^c*CNRS-Saint Gobain-NIMS, UMI 3629, Laboratory for Innovative Key Materials and Structures (LINK), National Institute for Materials Science (NIMS), Tsukuba, 305-0044, Japan*

#These authors contributed equally

I. Spectroscopic details

- Figure S1 ESI-MS spectrum of compound **2**.
- Figure S2 ^1H NMR spectrum of compound **2**.
- Figure S3 $^{11}\text{B}\{^1\text{H}\}$ NMR spectrum of compound **2**.
- Figure S4 $^{13}\text{C}\{^1\text{H}\}$ NMR spectrum of compound **2**.
- Figure S5 ESI-MS spectrum of compound **3**.
- Figure S6 ^1H NMR spectrum of compound **3**.
- Figure S7 $^{11}\text{B}\{^1\text{H}\}$ NMR spectrum of compound **3**.
- Figure S8 $^{13}\text{C}\{^1\text{H}\}$ NMR spectrum of compound **3**.
- Figure S9 ESI-MS spectrum of compound **4**.
- Figure S10 ^1H NMR spectrum of compound **4**.
- Figure S11 $^{11}\text{B}\{^1\text{H}\}$ NMR spectrum of compound **4**.
- Figure S12 $^{13}\text{C}\{^1\text{H}\}$ NMR spectrum of compound **4**.
- Figure S13 ESI-MS spectrum of compound **5**.
- Figure S14 ^1H NMR spectrum of compound **5**.
- Figure S15 $^{13}\text{C}\{^1\text{H}\}$ NMR spectrum of compound **5**.
- Figure S16 UV-Vis spectra of compounds **1b** and **2–4**.

II. Computational data

- Table S1 Selected bond parameters (\AA) and Wiberg bond indices (WBI) for the compounds **2'–5'** optimized at the B3LYP/def2-TZVP level.
- Table S2 Experimental and DFT calculated (B3LYP/Def2-TZVP) NMR chemical shifts δ (ppm) for compounds **2'–4'**.

Table S3	Calculated energies of the HOMO and LUMO (eV) and HOMO-LUMO gaps ($\Delta E = E_{\text{LUMO}} - E_{\text{HOMO}}$, eV) for compounds 1b' , 2–5' .
Table S4	Calculated natural charges (q) and natural valence population (pop) for compounds 1b' , 2–5' .
Table S5	Bond critical point properties computed at the B3LYP/Def2-TZVP level of theory of selected bonds in 5' . ρ is the value of the electron density, $\nabla^2\rho(r)$ is the Laplacian of the electron density, and $H(r)$ is the local energy density of the electron density at the bond critical points.
Figure S17	Frontier molecular orbitals of 3' and 4' [isocontour values: ± 0.04 (e/bohr ³) ^{1/2}].
Figure S18	Selected bonding molecular orbitals of 5' (a and b) and their occupation and percentage of NBO on each atom obtained; NBO donor-acceptor interaction of LP of N to <i>d</i> orbitals of Ta in 5' (c and d) and corresponding second order perturbation energy values [isocontour values: ± 0.04 (e/bohr ³) ^{1/2}].
Figure S19	Absorption spectrum of 1b' computed at the TD-DFT-B3LYP/Def2-TZVP level of theory (ε in LM ⁻¹ cm ⁻¹).
Table S6	TD-DFT calculated energies (excitation energy (eV), λ_{calc} (nm)), oscillator strengths (<i>f</i>), main composition of the first UV-vis electronic excitations for 1' . Experimental absorption wavelengths (λ_{exp} , nm) of 1b are given for comparison.
Figure S20	Absorption spectra of 2' computed at the TD-DFT-B3LYP/Def2-TZVP level of theory (ε in LM ⁻¹ cm ⁻¹).
Table S7	TD-DFT calculated energies (excitation energy (eV), λ_{calc} (nm)), oscillator strengths (<i>f</i>), main composition of the first UV-vis electronic excitations for 2' . Experimental absorption wavelengths (λ_{exp} , nm) are given for comparison.
Figure S21	Absorption spectra of 3' computed at the TD-DFT-B3LYP/Def2-TZVP level of theory (ε in LM ⁻¹ cm ⁻¹).

Table S8	TD-DFT calculated energies (excitation energy (eV), λ_{calc} (nm)), oscillator strengths (f), main composition of the first UV-vis electronic excitations for 3' . Experimental absorption wavelengths (λ_{exp} , nm) are given for comparison.
Figure S22	Absorption spectra of 4' computed at the TD-DFT-B3LYP/Def2-TZVP level of theory (ε in $\text{LM}^{-1}\text{cm}^{-1}$).
Table S9	TD-DFT calculated energies (excitation energy (eV), λ_{calc} (nm)), oscillator strengths (f), main composition of the first UV-vis electronic excitations for 4' . Experimental absorption wavelengths (λ_{exp} , nm) are given for comparison.
Figure S23	Optimized geometry of 2' (total energy (T. E.) = -1727.910339 a. u.)
Figure S24	Optimized geometry of 3' (T. E. = -1404.934563 a. u.).
Figure S25	Optimized geometry of 4' (T. E. = -3240.754367 a. u.)
Figure S26	Optimized geometry of 5' (T. E = -2752.057313 a. u.).

I. Spectroscopic details

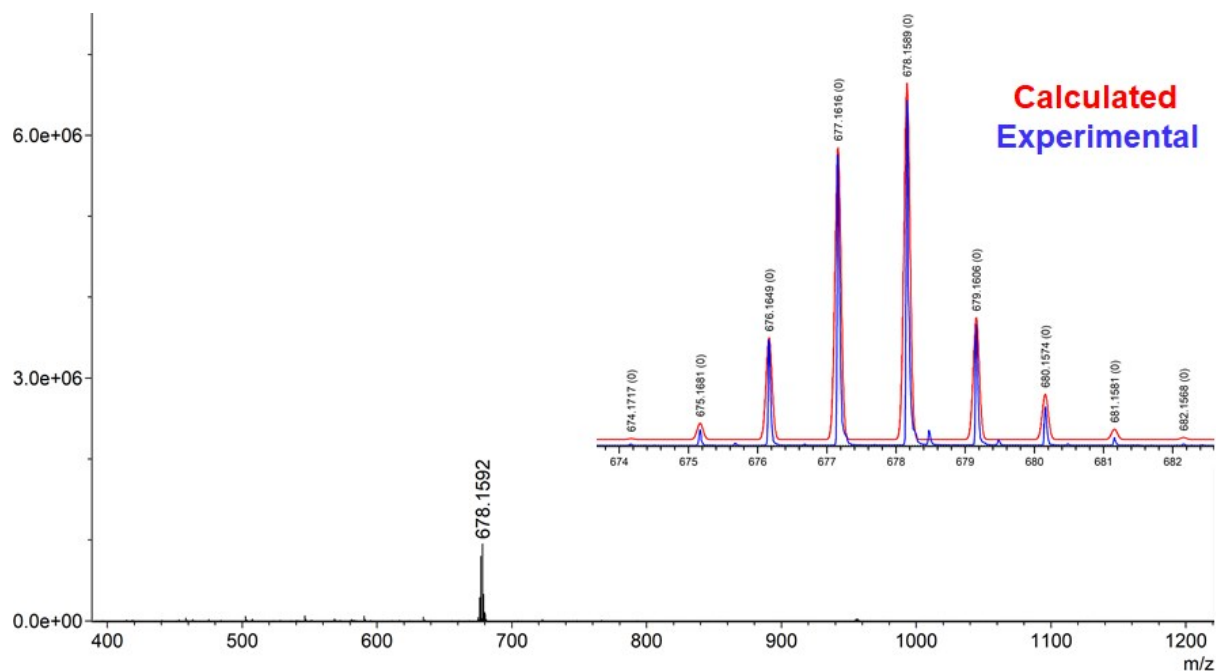


Figure S1. ESI-MS spectrum of compound **2**

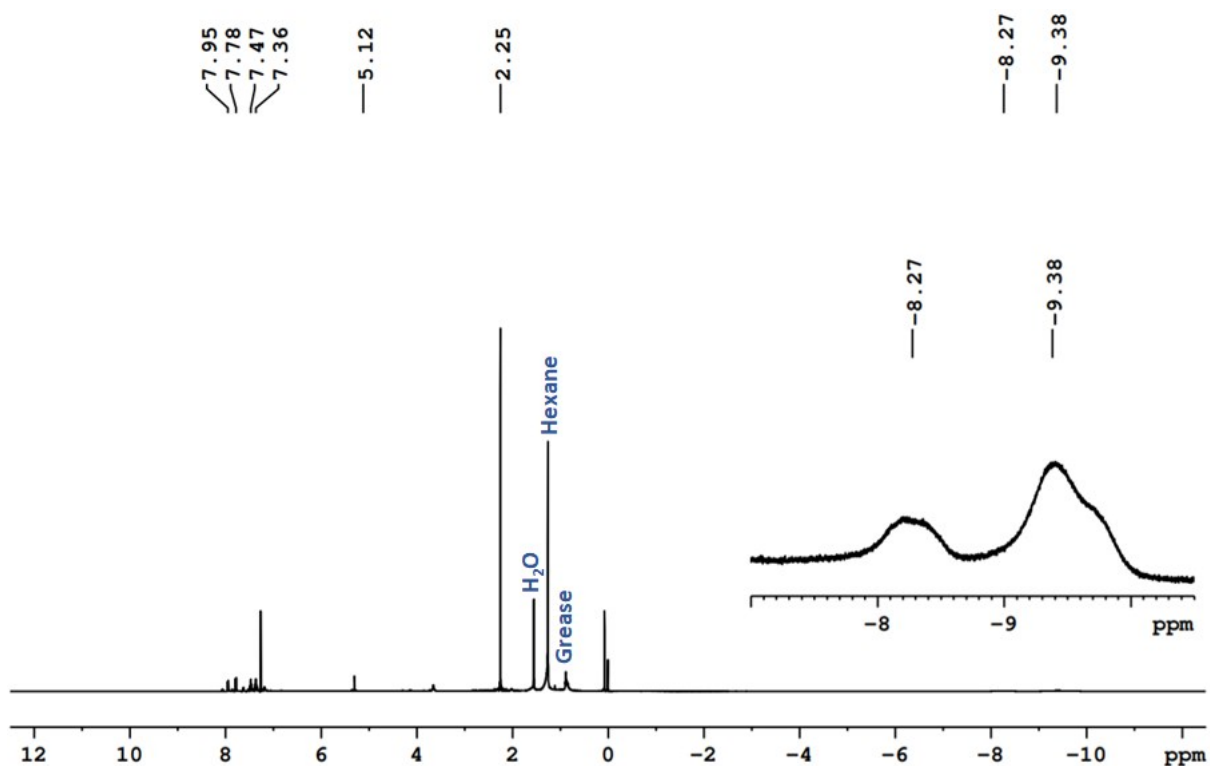


Figure S2. ¹H NMR spectrum of compound **2** in CDCl₃

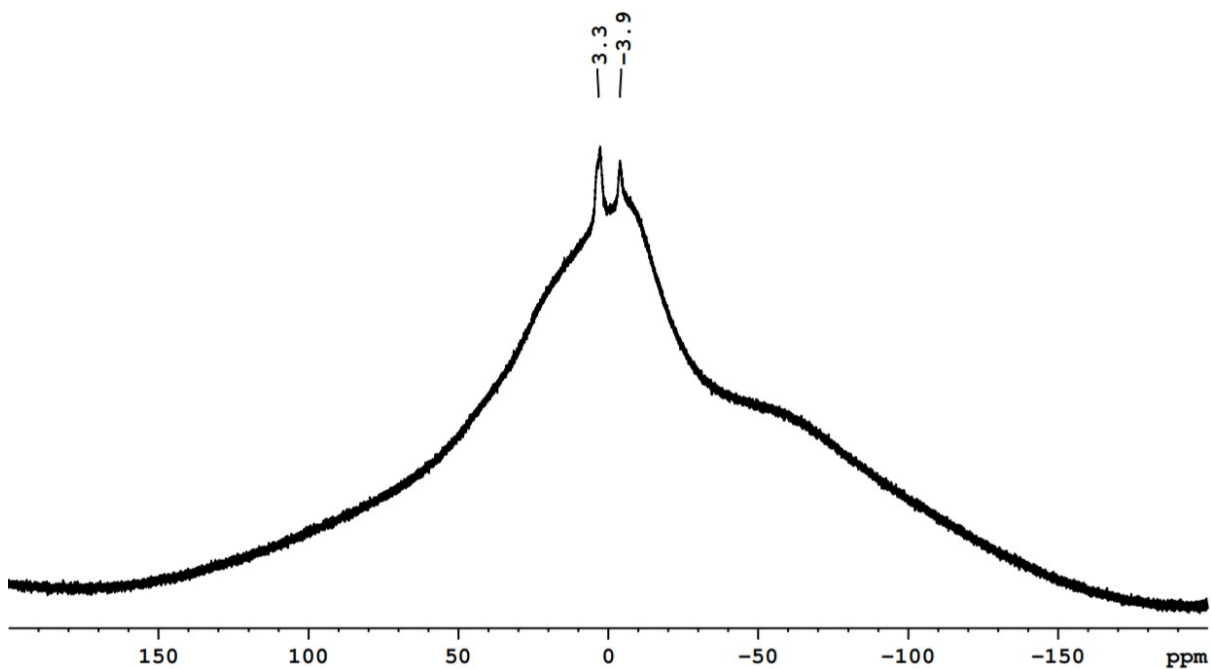


Figure S3. $^{11}\text{B}\{^1\text{H}\}$ NMR spectrum of compound **2** in CDCl_3

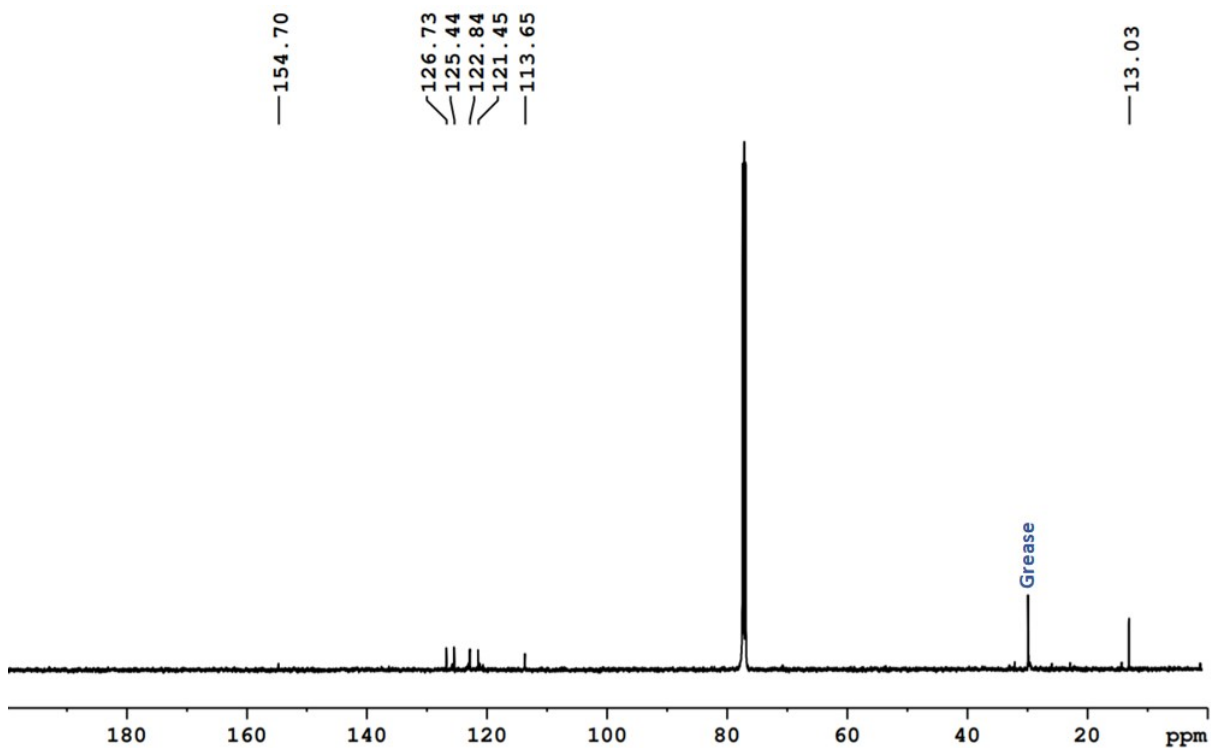


Figure S4. $^{13}\text{C}\{^1\text{H}\}$ NMR spectrum of compound **2** in CDCl_3

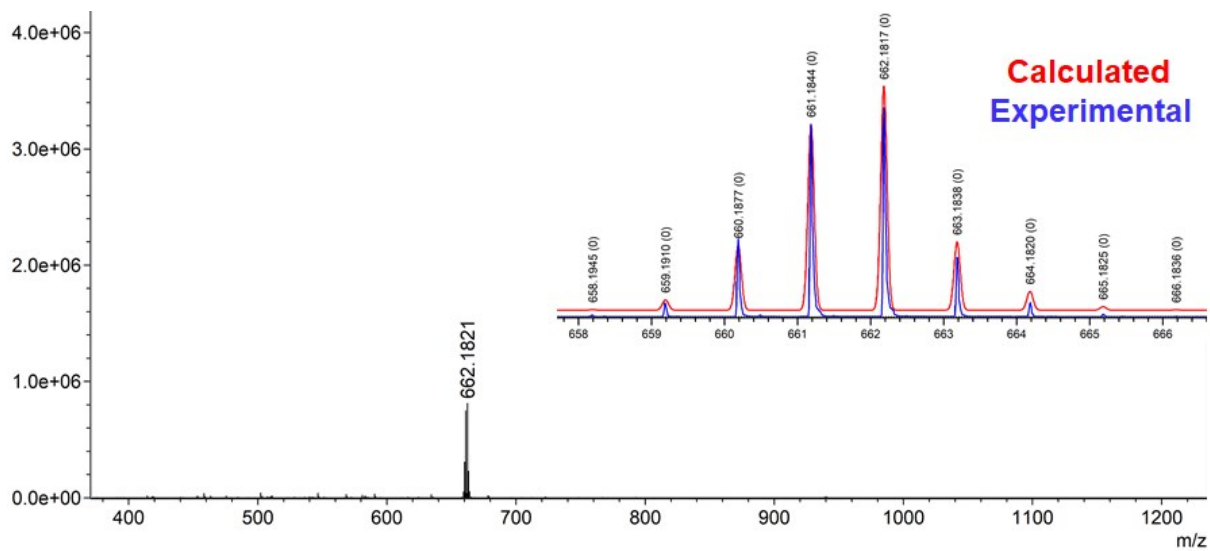


Figure S5. ESI-MS spectrum of compound 3

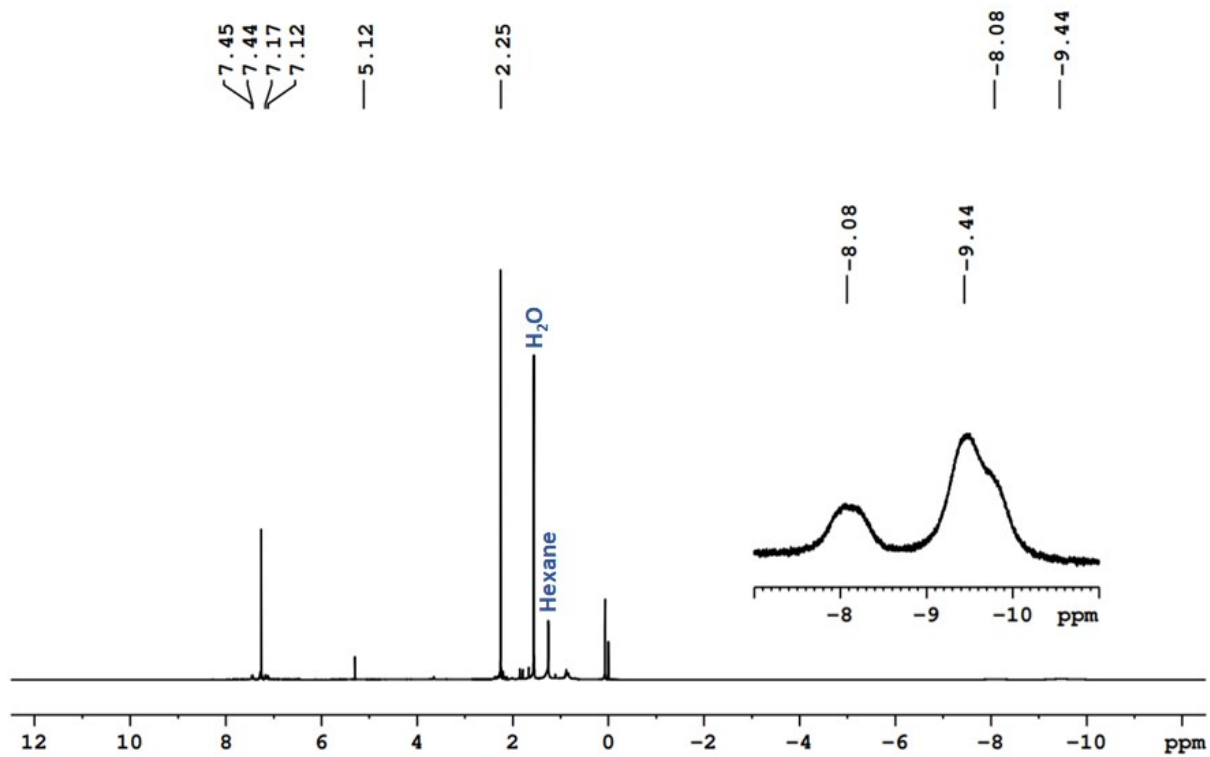


Figure S6. ^1H NMR spectrum of compound 3 in CDCl_3

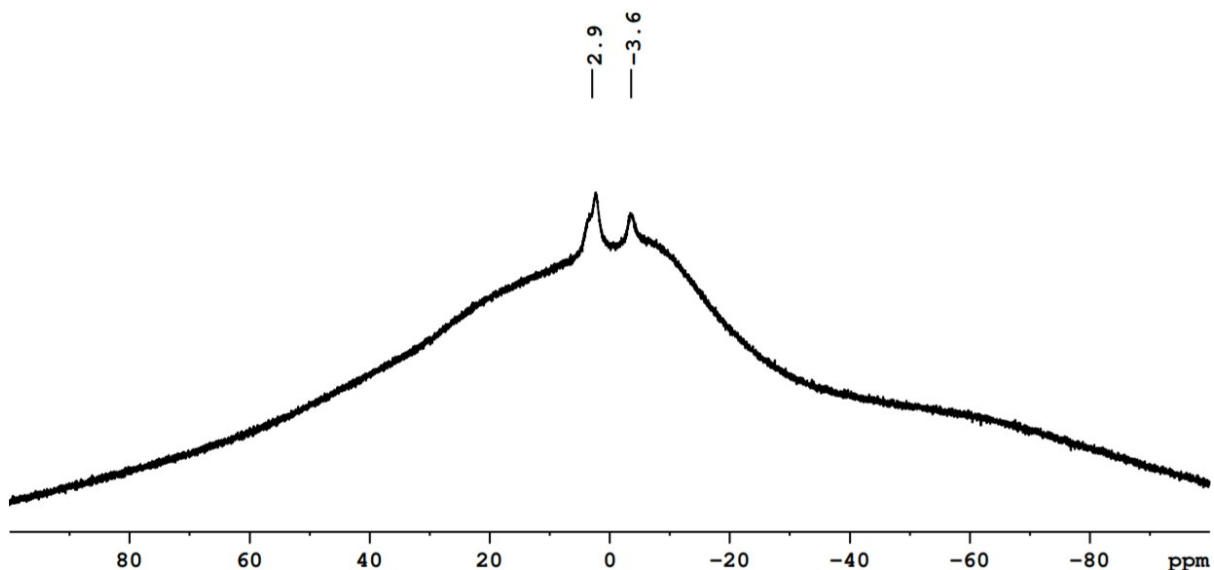


Figure S7. $^{11}\text{B}\{^1\text{H}\}$ NMR spectrum of compound **3** in CDCl_3

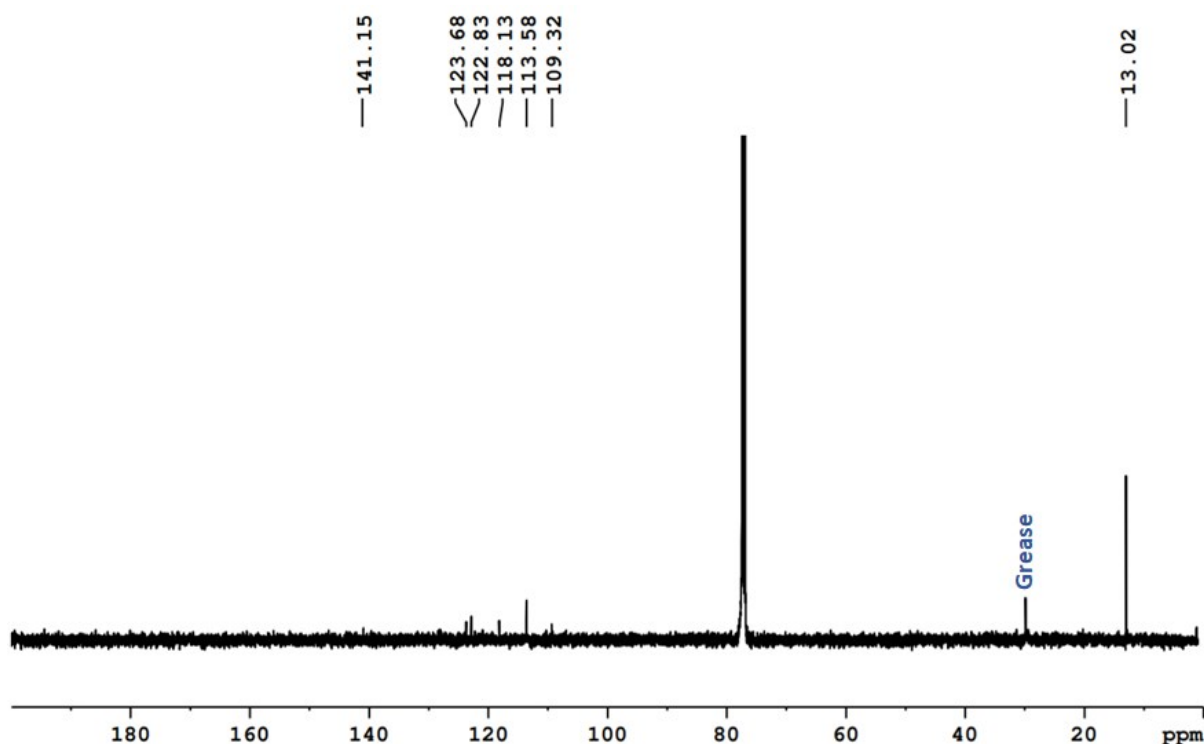


Figure S8. $^{13}\text{C}\{^1\text{H}\}$ NMR spectrum of compound **3** in CDCl_3

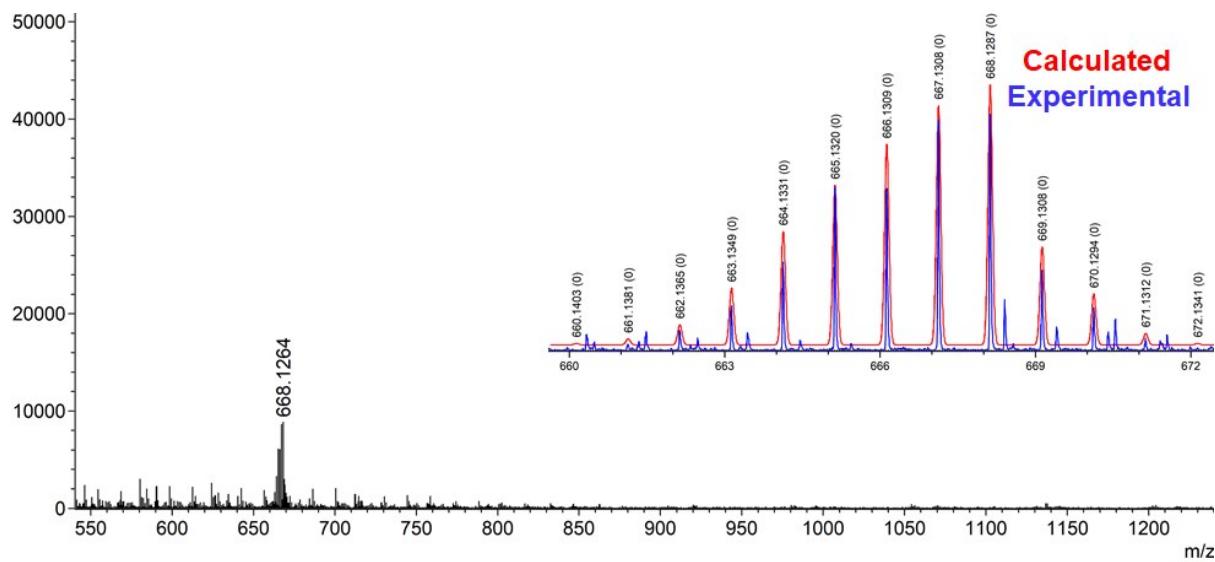


Figure S9. ESI-MS spectrum of compound **4**

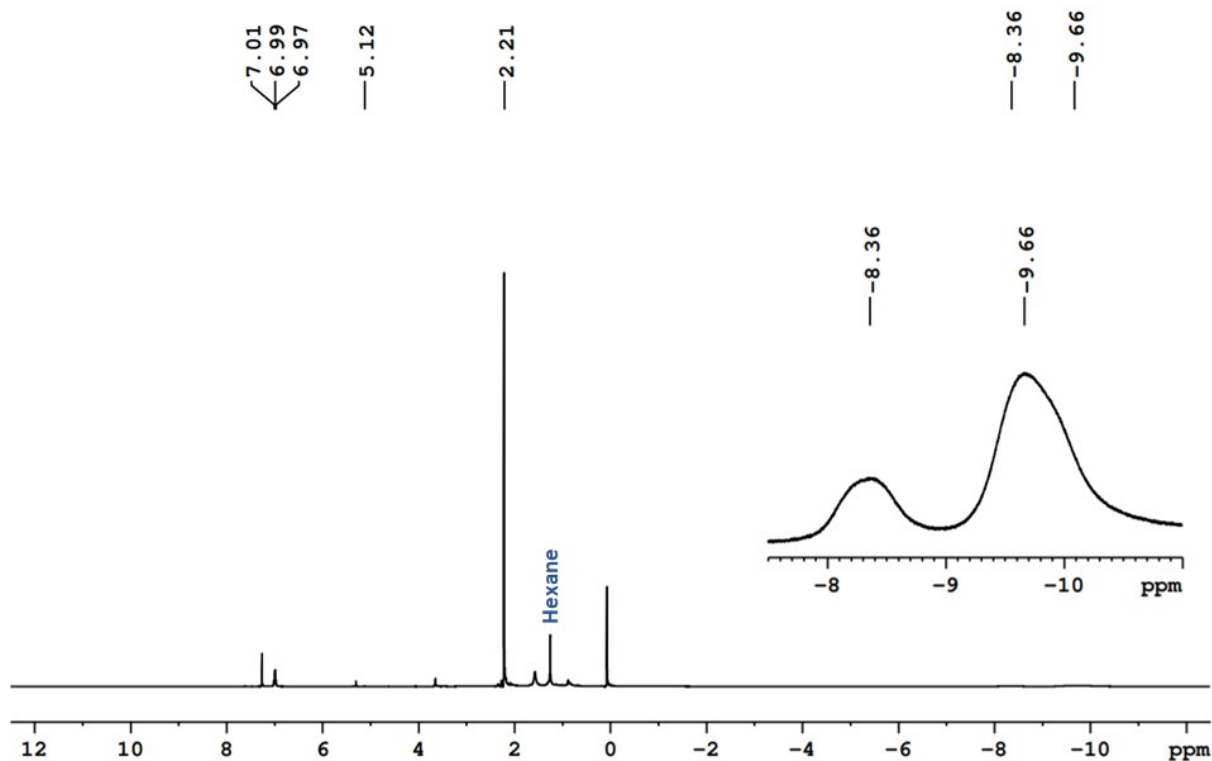


Figure S10. ^1H NMR spectrum of compound **4** in CDCl_3

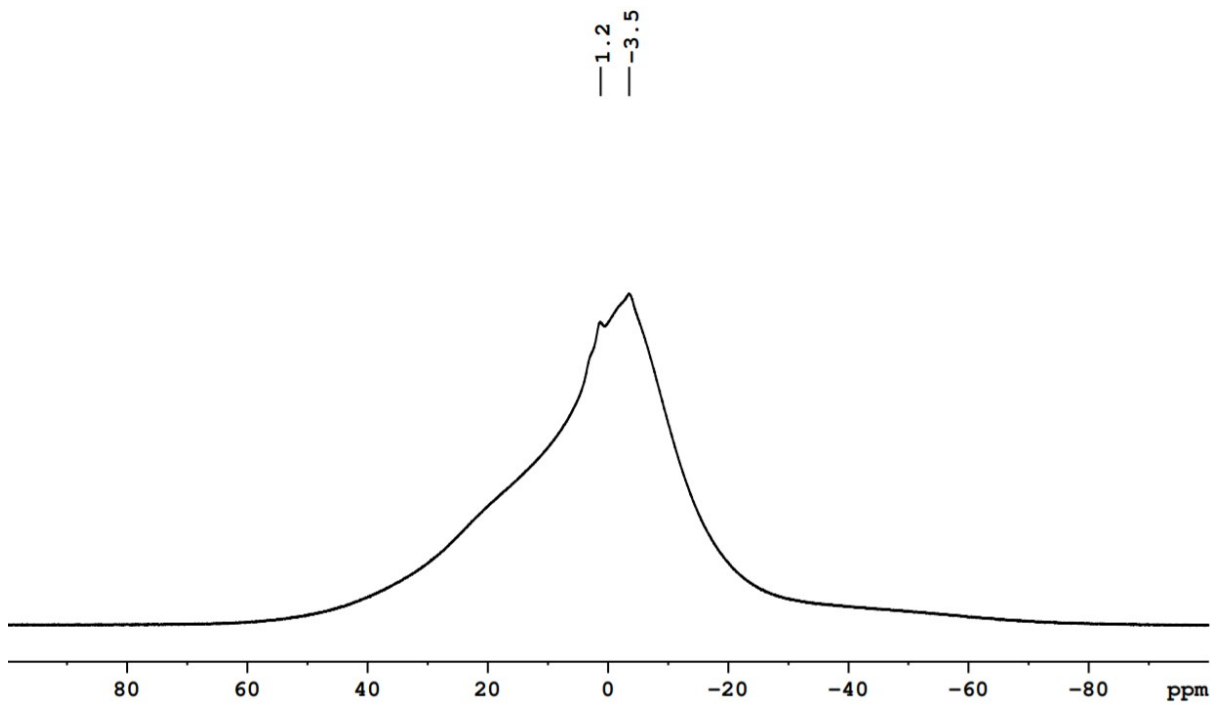


Figure S11. $^{11}\text{B}\{^1\text{H}\}$ NMR spectrum of compound **4** in CDCl_3

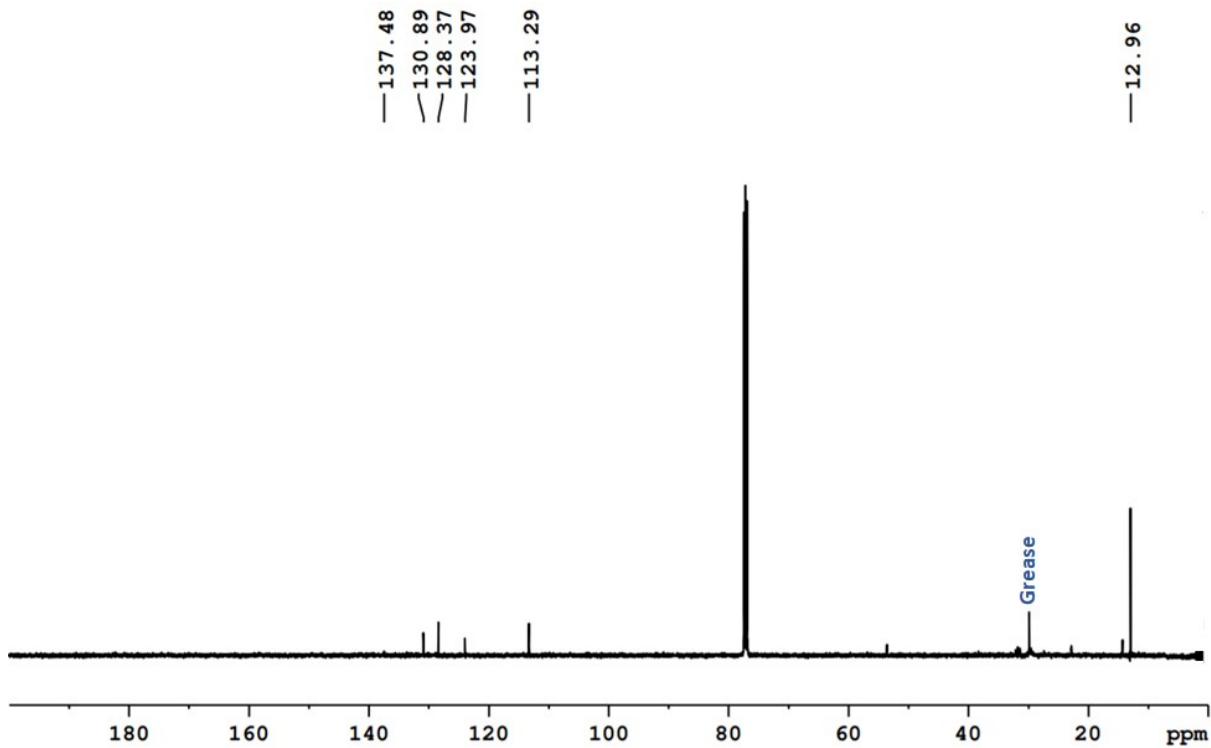


Figure S12. $^{13}\text{C}\{^1\text{H}\}$ NMR spectrum of compound **4** in CDCl_3

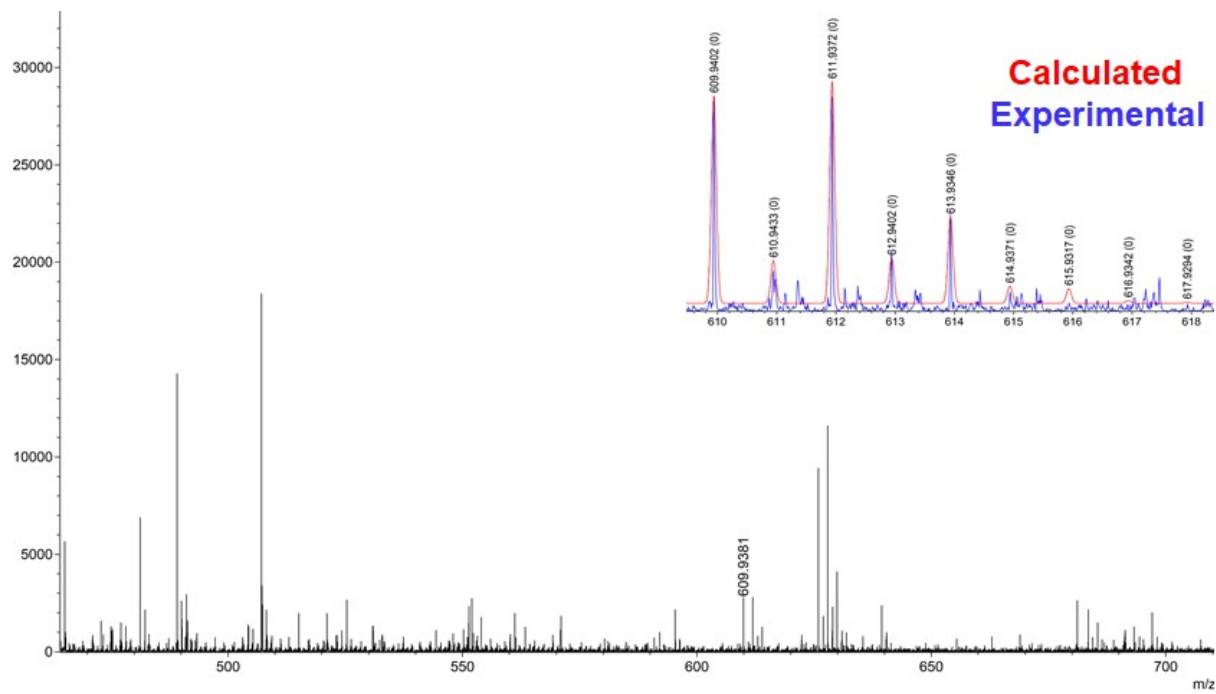


Figure S13. ESI-MS spectrum of compound 5

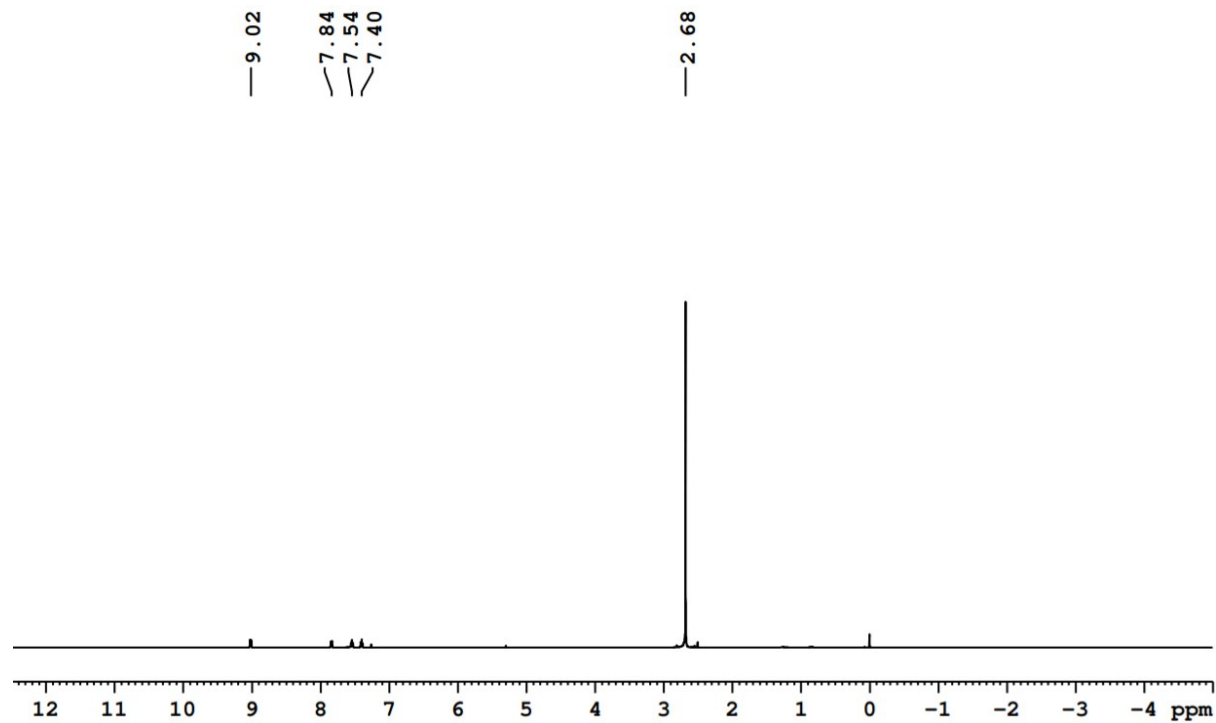


Figure S14. ^1H NMR spectrum of compound 5 in CDCl_3

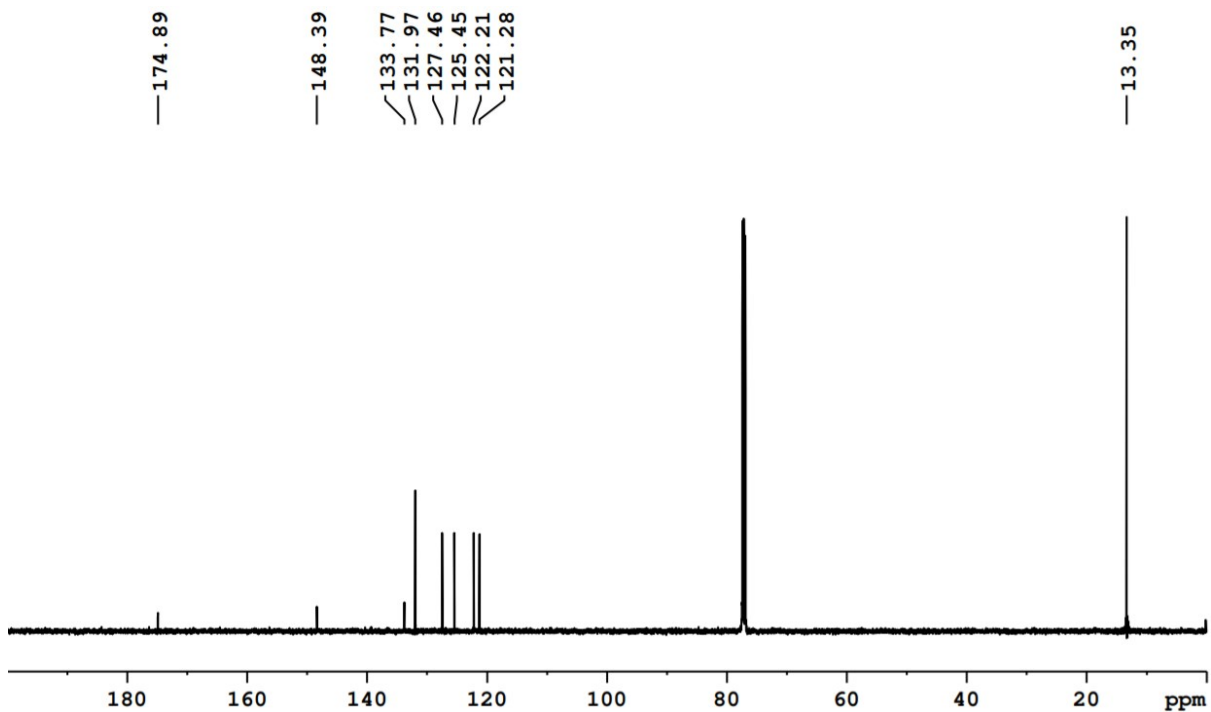


Figure S15. $^{13}\text{C}\{^1\text{H}\}$ NMR spectrum of compound **5** in CDCl_3

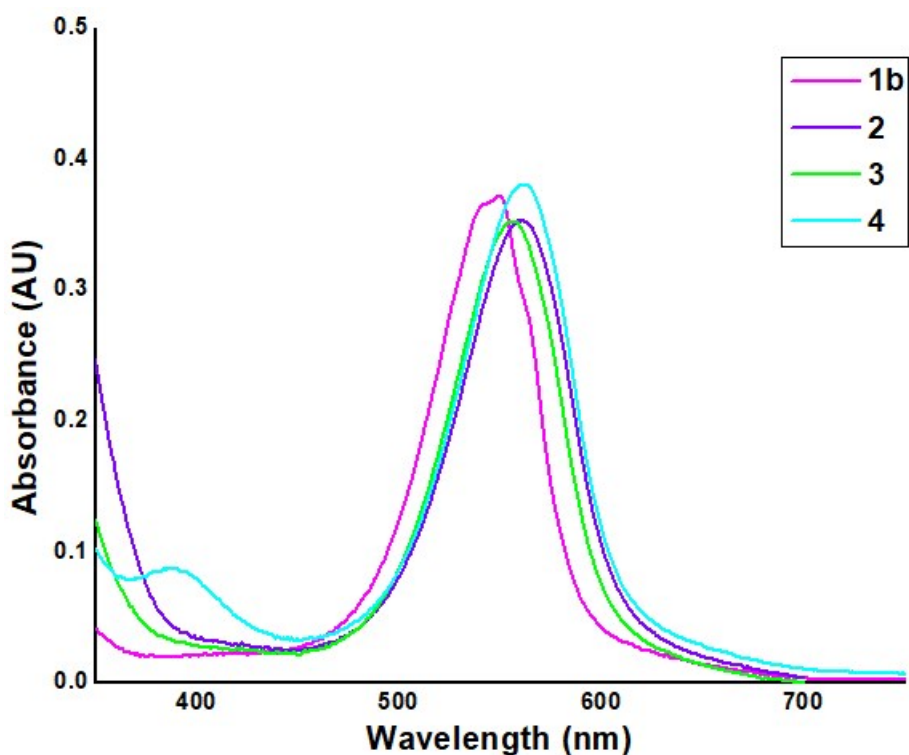


Figure S16. UV-Vis spectra of compounds **1b**, **2–4**

II. Computational data

Table S1. Selected bond parameters (\AA) and Wiberg bond indices (WBI) for the compounds **2'-5'** optimized at the B3LYP/def2-TZVP level.

	2'			3'			4'		
	Exp.	Cal.	WBI	Exp.	Cal.	WBI	Exp.	Cal.	WBI
Nb-Nb	2.960	2.965	1.01	2.957	2.965	1.01	2.956	2.961	1.01
B1-B2	1.777	1.781	0.61	1.799	1.781	0.61	1.777	1.779	0.61
B2-B3	1.775	1.797	0.55	1.778	1.797	0.55	1.794	1.796	0.55
Nb-B1	2.408	2.427	0.45	2.379	2.420	0.45	2.408	2.422	0.45
Nb-B2	2.416	2.424	0.46	2.399	2.422	0.47	2.421	2.423	0.47
Nb-B3	2.393	2.398	0.50	2.411	2.399	0.50	2.409	2.400	0.50
Nb-B4	2.399	2.399	0.50	2.393	2.400	0.50	2.407	2.402	0.50
B-S/Se	1.903	1.899	1.02	1.910	1.905	1.01	2.029	2.039	1.03

	5'		
	Exp.	Cal.	WBI
Ta-Cl1	2.414	2.429	1.14
Ta-Cl2	2.398	2.405	1.15
Ta-Cl3	2.407	2.429	1.14
Ta-S1	2.517	2.576	0.93
Ta-N	2.281	2.298	0.47

Table S2. Experimental and DFT calculated (B3LYP/Def2-TZVP) NMR chemical shifts δ (ppm) for compounds **2'-4'**.

	2'		3'		4'	
	Exp.	Calc.	Exp.	Calc.	Exp.	Calc.
B1	3.3	5.35	2.9	5.58	1.2	8.83
B2	-3.9	-3.49	-3.6	-3.49	-3.5	-3.47
B3	3.3.	8.86	2.9	8.19	1.2	6.72
B4	3.3	9.11	2.9	8.32	1.2	7.31

Table S3. Calculated energies of the HOMO and LUMO (eV) and HOMO-LUMO gaps ($\Delta E = E_{\text{LUMO}} - E_{\text{HOMO}}$, eV) for compounds **1b'** and **2'-5'**.

	1b'	2'	3'	4'	5'
HOMO	-5.08	-5.30	-5.32	-5.09.	-6.38
LUMO	-2.29	-2.67	-2.65	-2.55	-3.23
E	2.79	2.63	2.67	2.54	3.15

Table S4. Calculated natural charges (q) and natural valence population (pop) for compounds **1b'** and **2'-5'**.

	1b'		2'		3'		4'	
	<i>q</i>	pop	<i>q</i>	pop	<i>q</i>	pop	<i>q</i>	pop
Nb	-0.482	-5.450	-0.403	5.369	-0.403	5.370	-0.405	5.372
B1	-0.227	-3.198	-0.204	3.170	-0.182	3.147	-0.234	3.197
B2	-0.225	-3.195	-0.242	3.214	-0.246	3.218	-0.242	3.213
B3	-0.221	-3.191	-0.207	3.177	-0.208	3.178	-0.211	3.182
B4	-0.218	-3.188	-0.206	3.176	-0.208	3.178	-0.207	3.177
S/Se			0.218	5.746	0.192	5.779	0.225	5.759

5'		
	<i>q</i>	pop
Ta	0.331	4.503
Cl1	-0.189	7.172
Cl2	-0.180	7.163
Cl3	-0.189	7.172
S1	0.128	5.840
N	-0.462	5.425

Table S5. Bond critical point (bcp) properties computed at the B3LYP/Def2-TZVP level of theory of selected bonds in **5'**. ρ is the value of the electron density, $\nabla^2\rho(r)$ is the Laplacian of the electron density, and $H(r)$ is the local energy density of the electron density at the bcp's.

bond	$\rho(r)$	$\nabla^2\rho(r)$	$H(r)$
Ta-Cl1	0.0706	0.1783	-0.0166
Ta-S1	0.0675	0.0564	-0.0219
Ta-N	0.0420	0.3423	-0.0025

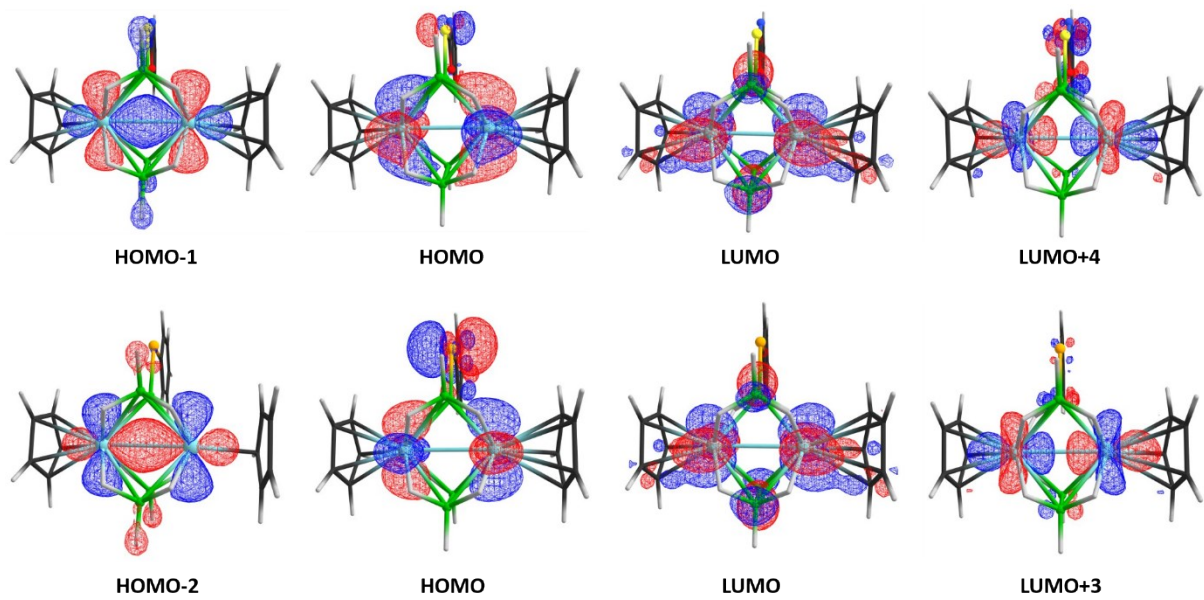


Figure S17. Frontier molecular orbitals of **3'**(top) and **4'**(bottom) [isocontour values: ± 0.04 ($e/\text{bohr}^3\right)^{1/2}$].

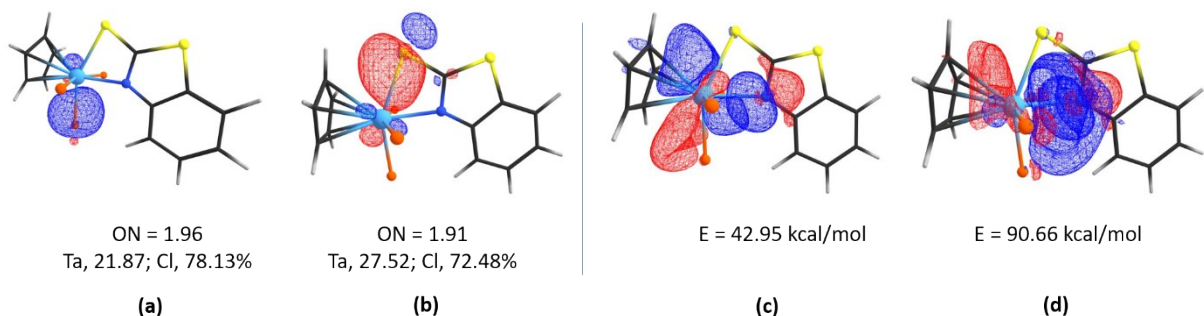


Figure S18. Selected bonding molecular orbital diagrams, of **5'** (a and b) and their occupation and percentage of NBO on each atom obtained; NBO donor-acceptor interaction of LP of N to LP* of Ta in **5'** (c and d) and corresponding stabilization energy(E) values [isocontour values: ± 0.04 ($e/\text{bohr}^3\right)^{1/2}$].

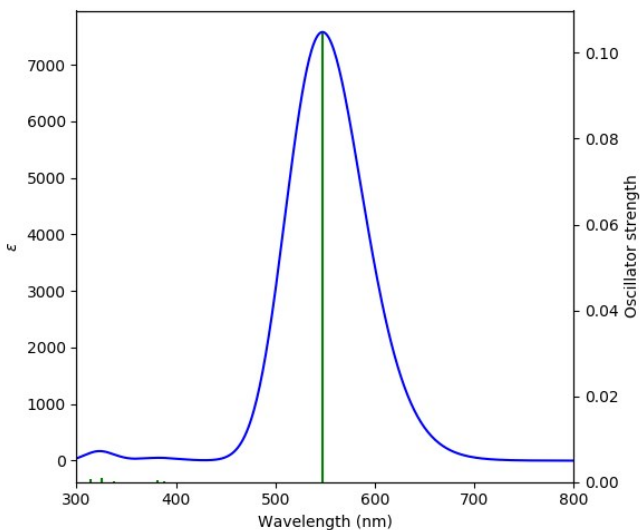


Figure S19. Absorption spectrum of **1b'** computed at the TD-DFT-B3LYP/Def2-TZVP level of theory (ϵ in $\text{LM}^{-1}\text{cm}^{-1}$).

Table S6. TD-DFT calculated energies (excitation energy (eV), λ_{calc} (nm)), oscillator strength (f), and main composition of the first UV-vis electronic excitations for **1b'**. Experimental absorption wavelengths (λ_{exp} , nm) of **1b** are given for comparison.

No	Excitation Energy (eV)	Wavelength λ (nm)		Main electronic transition (% weight) ^[a]
		Calc. (f)	Expt.	
1	1.859	667 (0.0)		HOMO-1→LUMO (99)
2	2.264	548 (0.10)	550	HOMO→LUMO (92)
3	2.853	435 (0.0)		HOMO→LUMO+1 (55)
				HOMO→LUMO+2 (43)
4	2.947	421 (0.00)		HOMO→LUMO+1 (43)
				HOMO→LUMO+2 (56)
5	3.195	388 (0.00)		HOMO-1→LUMO+1 (97)
6	3.247	382 (0.00)		HOMO-1→LUMO+2 (96)
7	3.670	338 (0.00)		HOMO-5→LUMO (93)
8	3.806	326 (0.00)		HOMO-1→LUMO+6 (15)
				HOMO→LUMO+4 (66)
				HOMO→LUMO+5 (15)

9	3.815	325 (0.00)	HOMO-1→LUMO+4 (49) HOMO-1→LUMO+5 (13) HOMO→LUMO+6 (35)
10	3.948	314 (0.00)	HOMO→LUMO+4 (17) HOMO→LUMO+5 (74)

[a]Components with greater than 10% contribution shown

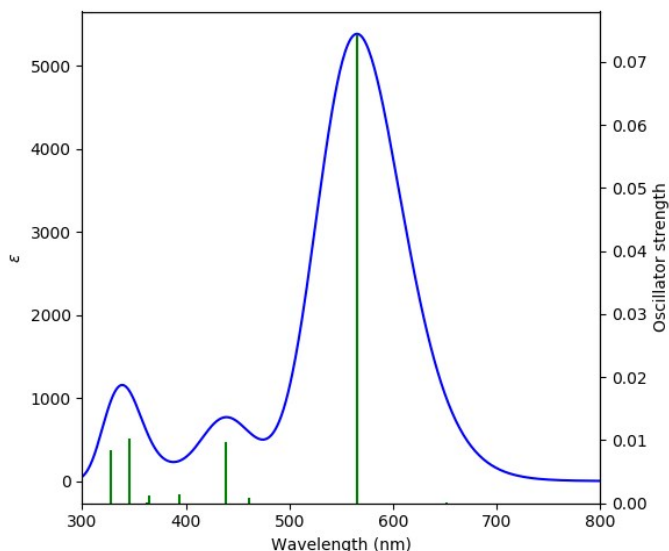


Figure S20. Absorption spectra of **2'** computed at the TD-DFT-B3LYP/Def2-TZVP level of theory (ϵ in $\text{LM}^{-1}\text{cm}^{-1}$).

Table S7. TD-DFT calculated energies (excitation energy (eV), λ_{calc} (nm)), oscillator strengths (f), main composition of the first UV-vis electronic excitations for **2'**. Experimental absorption wavelengths (λ_{exp} , nm) are given for comparison.

No	Excitation Energy (eV)	Wavelength (λ , nm)		Main electronic transition (% weight) [a]
		Calc. (f)	Exp.	
1	1.901	652 (0.00)		HOMO-1→LUMO (99)
2	2.193	564 (0.07)	560	HOMO→LUMO (93)
3	2.689	461 (0.00)		HOMO→LUMO+1 (90)
4	2.827	439 (0.01)		HOMO-2→LUMO+3 (97)
5	2.982	416 (0.0)		HOMO→LUMO+2 (91)

6	3.151	393 (0.00)	HOMO-1→LUMO+1 (97)
7	3.397	365 (0.00)	HOMO-1→LUMO+2 (96)
8	3.421	362 (0.00)	HOMO-3→LUMO (99)
9	3.589	345 (0.01)	HOMO→LUMO+3 (30)
			HOMO→LUMO+4 (59)
10	3.780	328 (0.01)	HOMO→LUMO+6 (62)

[a]Components with greater than 10% contribution shown

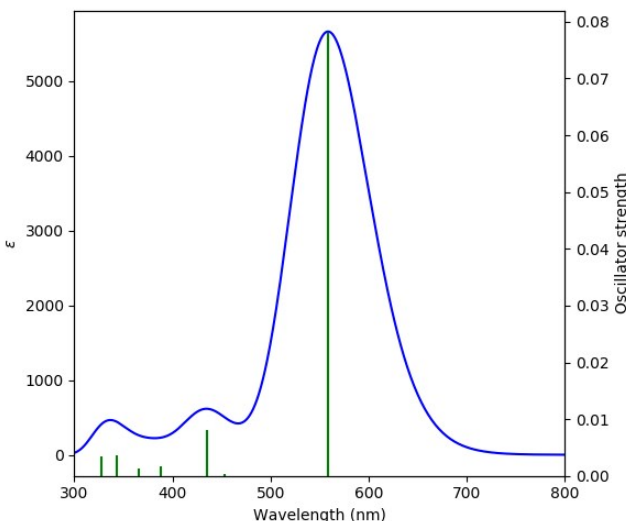


Figure S21. Absorption spectrum of **3'** computed at the TD-DFT-B3LYP/Def2-TZVP level of theory (ϵ in $\text{LM}^{-1}\text{cm}^{-1}$).

Table S8. TD-DFT calculated energies (excitation energy (eV), λ_{calc} (nm)), oscillator strengths (f), main composition of the first UV-vis electronic excitations for **3'**. Experimental absorption wavelengths (λ_{exp} , nm) are given for comparison.

No	Excitation Energy (eV)	Wavelength (λ , nm)		Main electronic transition (% weight) ^[a]
		Calc. (f)	Exp.	
1	1.913	648 (0.01)		HOMO-1→LUMO (99)
2	2.218	559 (0.08)	556	HOMO→LUMO (93)
3	2.737	453 (0.00)		HOMO→LUMO+1 (88)
4	2.851	435 (0.01)		HOMO-2→LUMO (97)
5	2.985	415 (0.0)		HOMO→LUMO+2 (88)

6	3.196	388 (0.00)	HOMO-1→LUMO+1 (97)
7	3.392	365 (0.00)	HOMO-1→LUMO+2 (96)
8	3.616	343 (0.00)	HOMO→LUMO+3 (28)
			HOMO→LUMO+4 (64)
9	3.771	329 (0.0)	HOMO-3→LUMO (100)
10	3.790	327 (0.00)	HOMO→LUMO+6 (80)

[a]Components with greater than 10% contribution shown

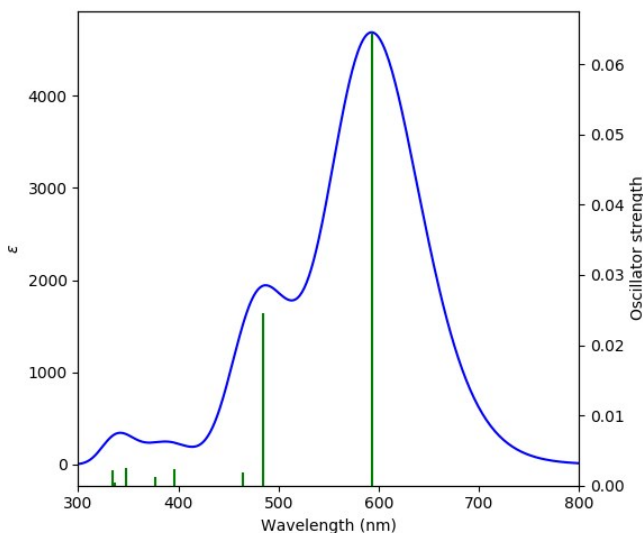


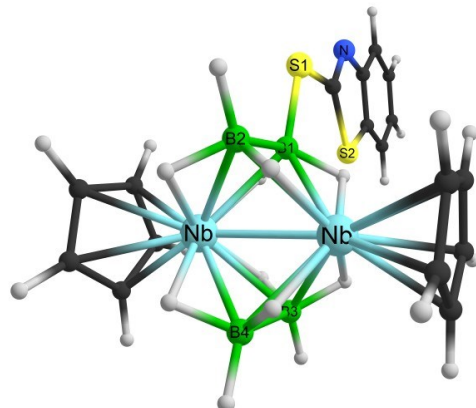
Figure S22. Absorption spectrum of **4'** computed at the TD-DFT-B3LYP/Def2-TZVP level of theory (ϵ in $\text{LM}^{-1}\text{cm}^{-1}$).

Table S9. TD-DFT calculated energies (excitation energy (eV), λ_{calc} (nm)), oscillator strengths (f), main composition of the first UV-vis electronic excitations for **4'**. Experimental absorption wavelengths (λ_{exp} , nm) are given for comparison.

No	Excitation Energy (eV)	Wavelength (λ , nm)		Main electronic transition (% weight) ^[a]
		Calc. (f)	Exp.	
1	1.844	672 (0.0)		HOMO-1→LUMO (99)
2	2.088	594 (0.06)	560	HOMO→LUMO (93)
3	2.556	485 (0.02)		HOMO-2→LUMO (96)
4	2.670	464 (0.00)		HOMO→LUMO+1 (86)
5	2.888	429 (0.0)		HOMO→LUMO+2 (87)

6	3.127	397 (0.00)	388	HOMO-1→LUMO+1 (97)
7	3.293	376 (0.00)		HOMO-1→LUMO+2 (97)
8	3.567	348 (0.00)		HOMO→LUMO+3 (57)
				HOMO→LUMO+4 (17)
				HOMO→LUMO+5 (16)
9	3.684	337 (0.00)		HOMO-2→LUMO+1 (94)
10	3.713	334 (0.00)		HOMO-1→LUMO+6 (14)
				HOMO→LUMO+5 (11)
				HOMO→LUMO+7 (52)

[a]Components with greater than 10% contribution shown

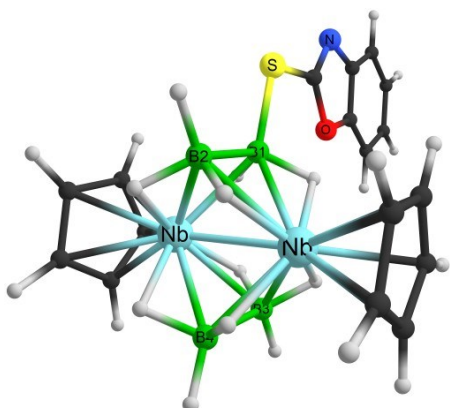


C	-1.997964000	-3.650639000	1.087920000
C	-3.045629000	-3.579058000	0.130230000
C	-2.461269000	-3.538460000	-1.163507000
C	-1.049154000	-3.561097000	-0.995427000
C	-0.770361000	-3.640254000	0.397225000
C	-1.022785000	3.557897000	-0.974347000
C	-0.778901000	3.636888000	0.425157000
C	-2.023924000	3.652200000	1.084110000
C	-3.047052000	3.585068000	0.100302000
C	-2.430847000	3.541248000	-1.177729000

C	2.718794000	-0.000792000	1.062736000
C	4.877597000	-0.000947000	0.579879000
C	6.256975000	-0.001118000	0.804413000
H	6.627381000	-0.001298000	1.820958000
C	7.116911000	-0.001046000	-0.281309000
H	8.186779000	-0.001178000	-0.115644000
C	6.624263000	-0.000805000	-1.591493000
H	7.314927000	-0.000747000	-2.424965000
C	5.258232000	-0.000629000	-1.836719000
H	4.879917000	-0.000431000	-2.850700000
C	4.393627000	-0.000705000	-0.746737000
B	-1.963709000	0.000187000	-1.956450000
B	-3.487257000	0.000948000	-1.003165000
B	-0.183882000	-0.000174000	0.891476000
B	-1.693375000	0.000557000	1.836991000
N	3.909831000	-0.000987000	1.562089000
S	2.652604000	-0.000500000	-0.715495000
S	1.296544000	-0.000791000	2.080922000
Nb	-1.843991000	1.482813000	-0.075548000
Nb	-1.845402000	-1.482128000	-0.075194000
H	-2.163256000	-0.000082000	-3.135107000
H	-4.459312000	0.001137000	-1.698872000
H	-1.488439000	0.000914000	3.015835000
H	-1.164400000	0.989911000	-1.773255000
H	-1.165508000	-0.990623000	-1.773036000
H	-3.671945000	0.991121000	-0.203380000

H	-0.006852000	-0.987142000	0.099877000
H	-3.672677000	-0.987877000	-0.202281000
H	-0.005926000	0.985964000	0.099339000
H	-2.476040000	-0.995485000	1.665331000
H	-2.475039000	0.997654000	1.665075000
H	-0.315777000	-3.561196000	-1.785359000
H	-2.991302000	-3.512329000	-2.101207000
H	-4.101154000	-3.588307000	0.348982000
H	-2.120580000	-3.691832000	2.158367000
H	0.209201000	-3.671209000	0.847166000
H	-2.173891000	3.694028000	2.151058000
H	-4.107736000	3.596733000	0.292459000
H	-2.937477000	3.516334000	-2.128318000
H	-0.269937000	3.556400000	-1.745729000
H	0.188975000	3.664920000	0.899866000

Figure S23. Optimized geometry and coordinates of **2'** (total energy (T. E.) = -1727.910339 a.u.)

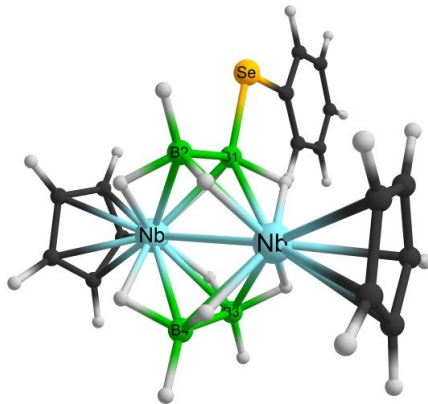


C	2.863872000	3.582222000	0.044941000
C	2.210334000	3.542014000	-1.215035000

C	0.809251000	3.561843000	-0.970541000
C	0.606456000	3.639068000	0.435381000
C	1.869806000	3.650737000	1.058195000
C	0.790417000	-3.558779000	-0.949594000
C	0.620987000	-3.636378000	0.461020000
C	1.899195000	-3.650978000	1.053029000
C	2.868671000	-3.584965000	0.016402000
C	2.185834000	-3.542439000	-1.227124000
C	-2.818500000	-0.000233000	1.234157000
C	-4.832601000	-0.000293000	0.551936000
C	-6.215795000	-0.000187000	0.400185000
H	-6.868070000	0.000309000	1.263103000
C	-6.718916000	-0.000741000	-0.896686000
H	-7.790654000	-0.000681000	-1.049492000
C	-5.874614000	-0.001376000	-2.013120000
H	-6.306354000	-0.001793000	-3.005534000
C	-4.487114000	-0.001486000	-1.874376000
H	-3.824659000	-0.001966000	-2.729211000
C	-4.013522000	-0.000944000	-0.578886000
B	1.690033000	0.000188000	-1.983800000
B	3.255398000	0.000385000	-1.101599000
B	0.047436000	-0.000136000	0.937281000
B	1.596311000	0.000172000	1.817114000
N	-4.029384000	0.000182000	1.687418000
S	-1.375384000	-0.000042000	2.203679000
Nb	1.656297000	-1.482072000	-0.097903000

Nb	1.655984000	1.482571000	-0.097926000
H	1.836169000	0.000204000	-3.170390000
H	4.193747000	0.000482000	-1.842216000
H	1.444053000	-0.000117000	3.004147000
H	0.900697000	-0.989711000	-1.764276000
H	0.900973000	0.990600000	-1.764576000
H	3.477327000	-0.989392000	-0.311772000
H	-0.170355000	0.983161000	0.154230000
H	3.476996000	0.989495000	-0.311154000
H	-0.170205000	-0.983158000	0.154165000
H	2.370921000	0.995861000	1.609857000
H	2.371446000	-0.995305000	1.609632000
O	-2.710176000	-0.000915000	-0.142860000
H	-0.320250000	-3.664841000	0.986511000
H	2.105589000	-3.691691000	2.110552000
H	3.938053000	-3.595750000	0.152146000
H	2.641492000	-3.518208000	-2.203187000
H	-0.001897000	-3.559245000	-1.680377000
H	-0.347109000	3.668734000	0.938116000
H	0.034359000	3.562808000	-1.719786000
H	2.688735000	3.517600000	-2.180143000
H	3.929715000	3.592367000	0.206042000
H	2.050519000	3.690919000	2.120412000

Figure S24. Optimized geometry and coordinates of **3'** (T. E. = -1404.934563 a. u.)

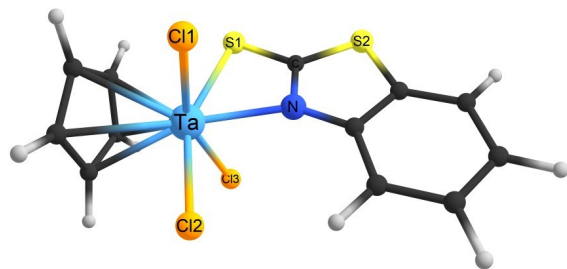


Nb	-1.405081000	1.480378000	0.078217000
C	-1.447997000	3.643558000	-1.108866000
C	-2.573885000	3.596977000	-0.244225000
C	-2.104679000	3.554751000	1.092822000
C	-0.681515000	3.553348000	1.047730000
C	-0.282429000	3.619633000	-0.317104000
Nb	-1.405090000	-1.480523000	0.077976000
C	-0.278530000	-3.621229000	-0.305380000
C	-1.435571000	-3.643714000	-1.109366000
C	-2.570467000	-3.595312000	-0.256543000
C	-2.115038000	-3.553951000	1.085618000
C	-0.691636000	-3.554543000	1.055139000
Se	2.187480000	0.000350000	-1.552720000
C	3.484342000	0.000129000	-0.122617000
C	3.159796000	-0.000077000	1.234202000
H	2.126185000	-0.000128000	1.551477000
C	4.164745000	-0.000216000	2.197497000
H	3.893379000	-0.000375000	3.246497000
C	5.502955000	-0.000150000	1.825042000
H	6.281419000	-0.000254000	2.577149000

C	5.830340000	0.000053000	0.472197000
H	6.869030000	0.000106000	0.164433000
C	4.832871000	0.000186000	-0.493016000
H	5.102144000	0.000341000	-1.542352000
B	0.392569000	0.000056000	-0.586057000
H	0.437224000	-0.987318000	0.220023000
H	0.437074000	0.986929000	0.220531000
B	-0.926375000	0.000144000	-1.779505000
H	-0.532155000	0.000324000	-2.909445000
H	-1.728749000	0.996273000	-1.743248000
H	-1.728736000	-0.995926000	-1.743433000
B	-1.850560000	-0.000199000	1.914143000
H	-2.250030000	-0.000439000	3.041282000
H	-1.033214000	-0.990978000	1.871956000
H	-1.033231000	0.990509000	1.872196000
B	-3.186485000	-0.000141000	0.712996000
H	-4.263944000	-0.000163000	1.231209000
H	-3.230954000	-0.990552000	-0.105614000
H	-3.230999000	0.990529000	-0.105435000
H	-2.734006000	-3.539091000	1.967471000
H	-3.599966000	-3.611240000	-0.576078000
H	-0.038766000	-3.555837000	1.912788000
H	0.739687000	-3.633794000	-0.660370000
H	-1.455661000	-3.677764000	-2.186887000
H	-3.606654000	3.613443000	-0.553033000
H	-2.714582000	3.540223000	1.980984000

H	-0.019889000	3.554308000	1.898638000
H	0.732031000	3.631232000	-0.682701000
H	-1.479482000	3.677736000	-2.186115000

Figure S25. Optimized geometry and coordinates of **4'** (T. E. = -3240.754367 a. u.)



Ta	-1.036764000	-0.094854000	0.000094000
Cl	-0.496293000	-0.133644000	-2.367805000
Cl	-0.496115000	-0.133322000	2.367872000
Cl	-0.640143000	-2.466639000	0.000242000
S	-0.211621000	2.345987000	-0.000085000
S	2.902240000	2.186769000	-0.000033000
C	-3.176354000	0.507737000	1.144572000
C	-3.294731000	-0.827038000	0.708359000
C	-3.294579000	-0.826808000	-0.709032000
C	-3.176161000	0.508116000	-1.144778000
C	-3.088935000	1.335920000	0.000031000
C	1.299037000	1.528754000	-0.000101000
N	1.240026000	0.218788000	-0.000127000
C	2.492157000	-0.380246000	-0.000081000
C	2.786657000	-1.743690000	-0.000128000
H	1.986363000	-2.466945000	-0.000174000
C	4.115498000	-2.135173000	-0.000109000

H	4.353842000	-3.190811000	-0.000143000
C	5.151854000	-1.196867000	-0.000050000
H	6.181031000	-1.531184000	-0.000036000
C	4.875193000	0.161851000	-0.000020000
H	5.673754000	0.891724000	0.000020000
C	3.543478000	0.559202000	-0.000033000
H	-3.331073000	-1.697435000	1.341318000
H	-3.330784000	-1.696998000	-1.342284000
H	-3.110719000	0.836160000	-2.166754000
H	-3.002928000	2.409468000	0.000217000
H	-3.111140000	0.835458000	2.166668000

Figure S26. Optimized geometry and coordinates of **5'** (T. E. = -2752.057313 a. u.).